

Disorder in quantum vacuum: Casimir-induced localization of matter waves

Diego A. R. Dalvit
Theoretical Division
Los Alamos National Laboratory



Collaborators



Gustavo Moreno (UBA - Buenos Aires)

Riccardo Messina (SYRTE - Paris)

Astrid Lambrecht (LKB - Paris)

Paulo Maia Neto (UFRJ - Rio de Janeiro)

Serge Reynaud (LKB - Paris)

Work recently published in PRL **105**, 210401 (2010)

Outline of this talk

- Review of theory and experiment on Casimir atom-surface interactions
- Casimir-Polder forces within scattering theory
- Cold atoms for probing geometry effects on CP forces
- Localization of matter waves induced by disordered CP

The Casimir-Polder force



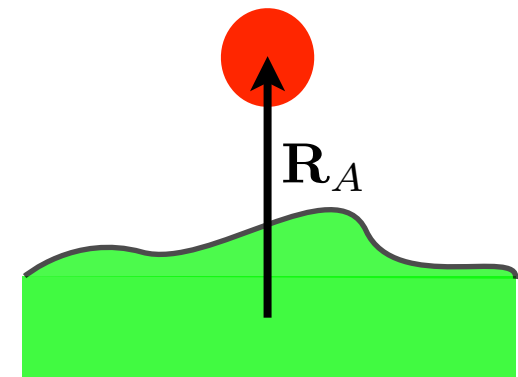
The Casimir-Polder force

vdW - CP interaction

Casimir and Polder (1948)

The interaction energy between a ground-state atom and a surface is given by

$$U_{\text{CP}}(\mathbf{R}_A) = \frac{\hbar}{c^2 \epsilon_0} \int_0^\infty \frac{d\xi}{2\pi} \xi^2 \alpha(i\xi) \text{Tr } \mathbf{G}(\mathbf{R}_A, \mathbf{R}_A, i\xi)$$



Atomic polarizability: $\alpha(\omega) = \lim_{\epsilon \rightarrow 0} \frac{2}{3\hbar} \sum_k \frac{\omega_{k0} |\mathbf{d}_{0k}|^2}{\omega_{k0}^2 - \omega^2 - i\omega\epsilon}$

Scattering Green tensor: $\left(\nabla \times \nabla \times -\frac{\omega^2}{c^2} \epsilon(\mathbf{r}, \omega) \right) \mathbf{G}(\mathbf{r}, \mathbf{r}', \omega) = \delta(\mathbf{r} - \mathbf{r}')$

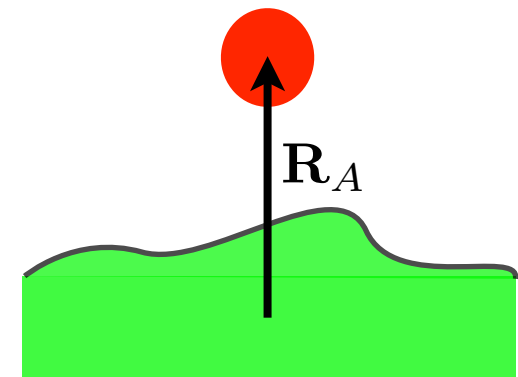
The Casimir-Polder force

■ vdW - CP interaction

Casimir and Polder (1948)

The interaction energy between a ground-state atom and a surface is given by

$$U_{\text{CP}}(\mathbf{R}_A) = \frac{\hbar}{c^2 \epsilon_0} \int_0^\infty \frac{d\xi}{2\pi} \xi^2 \alpha(i\xi) \text{Tr } \mathbf{G}(\mathbf{R}_A, \mathbf{R}_A, i\xi)$$



Atomic polarizability: $\alpha(\omega) = \lim_{\epsilon \rightarrow 0} \frac{2}{3\hbar} \sum_k \frac{\omega_{k0} |\mathbf{d}_{0k}|^2}{\omega_{k0}^2 - \omega^2 - i\omega\epsilon}$

Scattering Green tensor: $\left(\nabla \times \nabla \times -\frac{\omega^2}{c^2} \epsilon(\mathbf{r}, \omega) \right) \mathbf{G}(\mathbf{r}, \mathbf{r}', \omega) = \delta(\mathbf{r} - \mathbf{r}')$

■ Eg: Ground-state atom near planar surface @ T=0

Non-retarded (vdW) limit $z_A \ll \lambda_A$

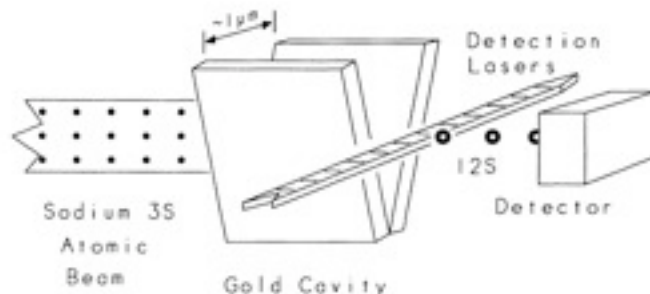
$$U_{\text{vdW}}(z_A) = -\frac{\hbar}{8\pi\epsilon_0} \frac{1}{z_A^3} \int_0^\infty \frac{d\xi}{2\pi} \alpha(i\xi) \frac{\epsilon(i\xi) - 1}{\epsilon(i\xi) + 1}$$

Retarded (CP) limit $z_A \gg \lambda_A$

$$U_{\text{CP}}(z_A) = -\frac{3\hbar c \alpha(0)}{8\pi} \frac{1}{z_A^4} \frac{\epsilon_0 - 1}{\epsilon_0 + 1} \phi(\epsilon_0)$$

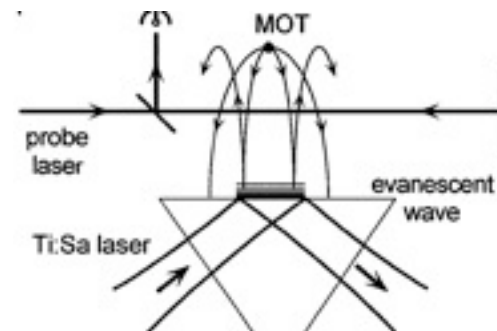
Modern CP experiments

Deflection of atoms

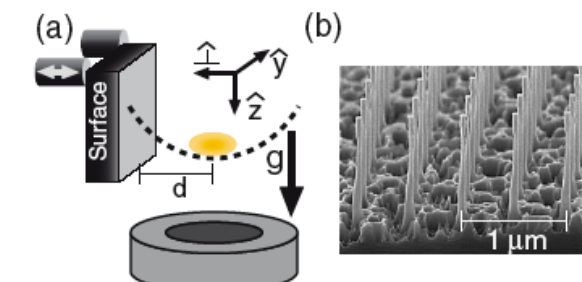


Hinds et al (1993)

Classical/quantum reflection

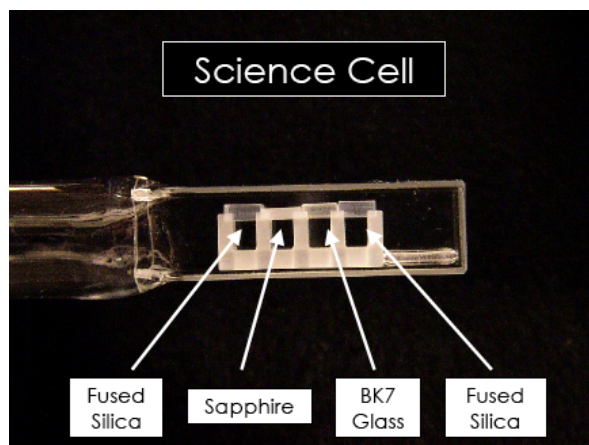


Aspect et al (1996)



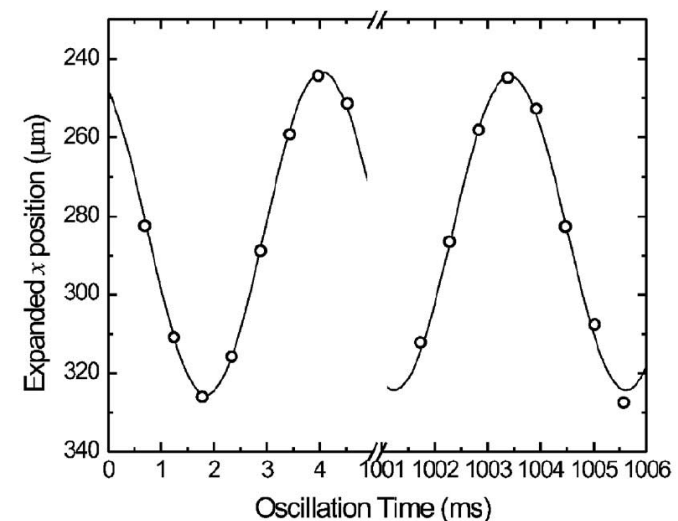
Ketterle et al (2006)

BEC oscillator



Cornell et al (2007)

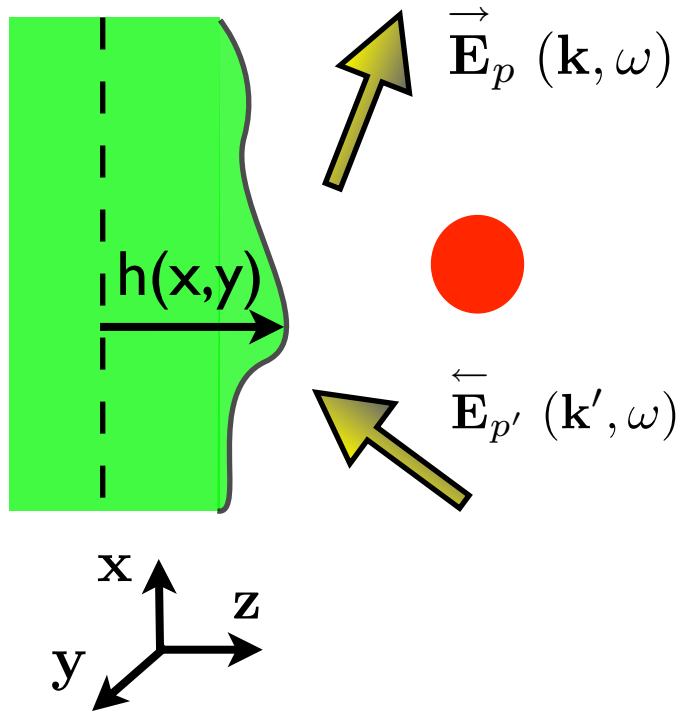
$$\gamma_x \equiv \frac{\omega_x - \omega'_x}{\omega_x} \approx -\frac{1}{2\omega_x^2 m} \partial_x^2 U^*$$



CP within scattering theory



CP within scattering theory



Output fields:

$$\vec{E}(\mathbf{R}, \omega) = \int \frac{d^2\mathbf{k}}{(2\pi)^2} e^{-i\mathbf{k}\cdot\mathbf{r}} \vec{E}(\mathbf{k}, z, \omega)$$

$$\vec{E}(\mathbf{k}, z, \omega) = [\vec{E}_{TE}(\mathbf{k}, \omega) \hat{\epsilon}_{TE}^+(\mathbf{k}) + \vec{E}_{TM}(\mathbf{k}, \omega) \hat{\epsilon}_{TM}^+(\mathbf{k})] e^{ik_z z}$$

$$\hat{\epsilon}_{TE}^+(\mathbf{k}) = \mathbf{z} \times \mathbf{k} \quad \hat{\epsilon}_{TM}^+(\mathbf{k}) = \hat{\epsilon}_{TE}^+(\mathbf{k}) \times \mathbf{K} \quad (\mathbf{K} = \mathbf{k} + k_z \mathbf{z})$$

Input fields: idem with $k_z \rightarrow -k_z$

Input and output fields related via reflection operators

$$\vec{E}_p(\mathbf{k}, \omega) = \int \frac{d^2\mathbf{k}'}{(2\pi)^2} \sum_{p'} \langle \mathbf{k}, p | \mathcal{R}(\omega) | \mathbf{k}', p' \rangle \vec{E}_{p'}(\mathbf{k}', \omega)$$

Casimir-Polder force:

$$U_{CP}(\mathbf{R}_A) = \frac{\hbar}{c^2 \epsilon_0} \int_0^\infty \frac{d\xi}{2\pi} \xi^2 \alpha(i\xi) \int \frac{d^2\mathbf{k}}{(2\pi)^2} \int \frac{d^2\mathbf{k}'}{(2\pi)^2} e^{i(\mathbf{k}-\mathbf{k}') \cdot \mathbf{r}_A} e^{-(\kappa+\kappa') z_A} \frac{1}{2\kappa'} \sum_{p,p'} \hat{\epsilon}_p^+(\mathbf{k}) \cdot \hat{\epsilon}_{p'}^-(\mathbf{k}') R_{p,p'}(\mathbf{k}, \mathbf{k}')$$

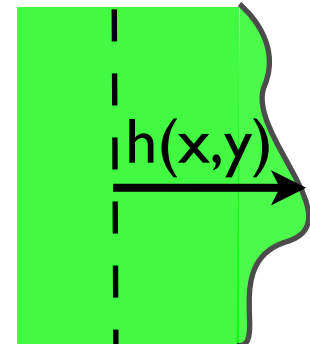
with $\kappa \equiv \sqrt{\xi^2/c^2 + k^2}$ and $R_{p,p'}(\mathbf{k}, \mathbf{k}')$ dependent on material properties at freq. $i\xi$

Specular/non specular scattering



In order to treat a general rough or corrugated surface, we make a perturbative expansion in powers of $h(x,y)$

$$\mathcal{R} = \mathcal{R}^{(0)} + \mathcal{R}^{(1)} + \mathcal{R}^{(2)} + \dots$$



□ Specular reflection:

$$\langle \mathbf{k}, p | \mathcal{R}^{(0)} | \mathbf{k}', p' \rangle = (2\pi)^2 \delta^{(2)}(\mathbf{k} - \mathbf{k}') \delta_{p,p'} r_p(\mathbf{k}, \xi)$$

Fresnel coefficients $r_{\text{TE}} = \frac{\kappa - \kappa_t}{\kappa + \kappa_t}$ $r_{\text{TM}} = \frac{\epsilon(i\xi)\kappa - \kappa_t}{\epsilon(i\xi)\kappa + \kappa_t}$ ($\kappa_t = \sqrt{\epsilon(i\xi)\xi^2/c^2 + k^2}$)

□ Non-specular reflection:

$$\langle \mathbf{k}, p | \mathcal{R}^{(1)} | \mathbf{k}', p' \rangle = R_{p,p'}(\mathbf{k}, \mathbf{k}') H(\mathbf{k} - \mathbf{k}') \quad \leftarrow \text{Fourier transform of } h(x,y)$$

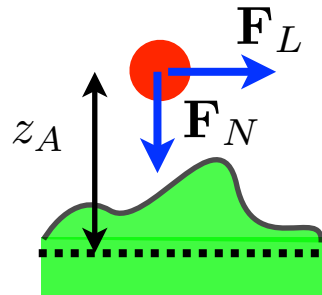


The non-specular reflection matrices depend on the geometry and material properties.

Probing geometry effects



Probing geometry effects



$$U_{\text{CP}} = U_{\text{CP}}^{(0)}(z_A) + U_{\text{CP}}^{(1)}(z_A, x_A)$$

■ **Normal CP force:**

$$U_{\text{CP}}^{(0)}(z_A) = \frac{\hbar}{c^2 \epsilon_0} \int_0^\infty \frac{d\xi}{2\pi} \xi^2 \alpha(i\xi) \int \frac{d^2\mathbf{k}}{(2\pi)^2} \frac{1}{2\kappa} \sum_p \hat{\epsilon}_p^+ \cdot \hat{\epsilon}_p^- r_p(\mathbf{k}, \xi) e^{-2\kappa z_A}$$

■ **Lateral CP force:**

$$U_{\text{CP}}^{(1)}(z_A, x_A) = \int \frac{d^2\mathbf{k}}{(2\pi)^2} e^{i\mathbf{k} \cdot \mathbf{r}_A} g(\mathbf{k}, z_A) H(\mathbf{k})$$

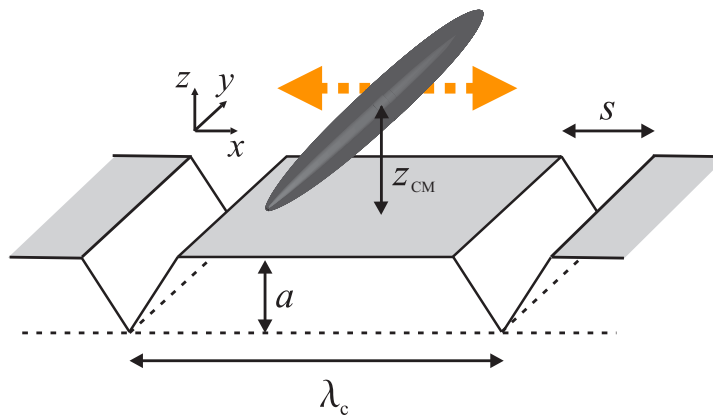
Response function g:

$$g(\mathbf{k}, z_A) = \frac{\hbar}{c^2 \epsilon_0} \int_0^\infty \frac{d\xi}{2\pi} \xi^2 \alpha(i\xi) \int \frac{d^2\mathbf{k}'}{(2\pi)^2} a_{\mathbf{k}', \mathbf{k}' - \mathbf{k}}(z_A, \xi)$$

$$a_{\mathbf{k}', \mathbf{k}''} = \sum_{p', p''} \hat{\epsilon}_{p'}^+ \cdot \hat{\epsilon}_{p''}^- \frac{e^{-(\kappa' + \kappa'') z_A}}{2\kappa''} R_{p', p''}(\mathbf{k}', \mathbf{k}'')$$

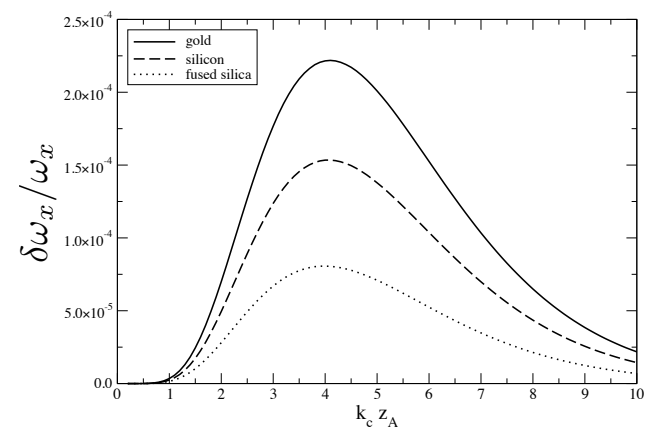
BEC as a “cantilever”

- In order to measure the lateral component $U_{\text{CP}}^{(1)}(x, z)$, a cigar-shaped BEC could be trapped parallel to the corrugation lines, and the **lateral dipolar oscillation** measured as a function of time



- Mean field BEC dynamics given by the Gross-Pitaevskii equation for the condensate wave-function φ

$$i\hbar\partial_t\varphi = -(\hbar^2/2m)\nabla^2\varphi + [U_N(z) + U_L(x, z)]\varphi + (m/2)(\omega_r^2 r^2 + \omega_x^2 x^2)\varphi + g|\varphi|^2\varphi,$$



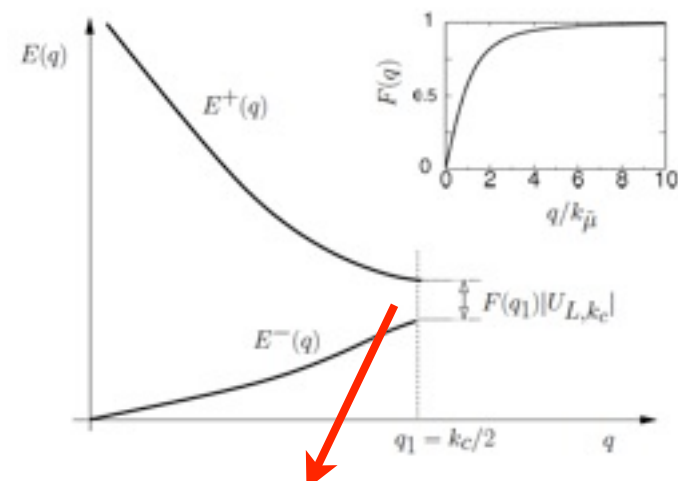
Dalvit et al (PRL 2008)

BEC Bragg spectroscopy

- The CP interaction also modifies the Bogoliubov spectrum of quantum fluctuations

$$E(q) = E_B(q) + \delta E_{CP}(q)$$

$$E_B(q) = \sqrt{(\hbar^2 q^2 / 2m)(\hbar^2 q^2 / 2m + 2\tilde{\mu})}$$



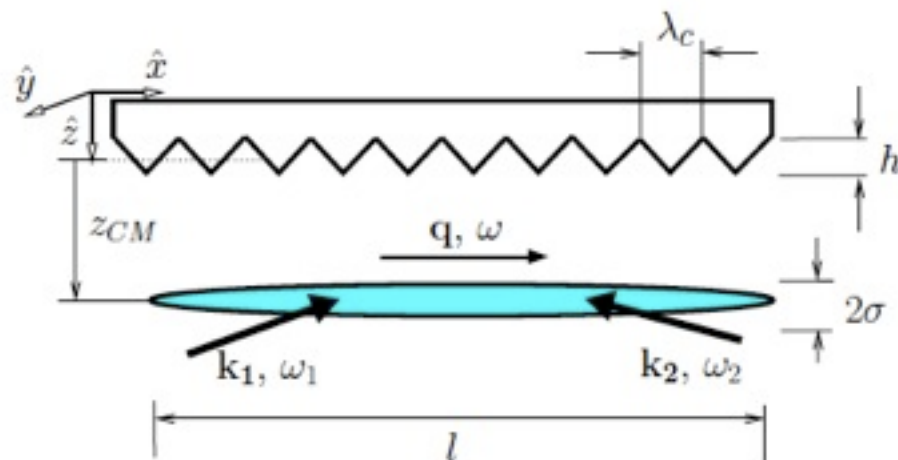
- Two-photon Bragg spectroscopy to measure the dynamic structure factor, and hence the spectrum

$$\begin{aligned} \frac{dP_X}{dt} &= -m\omega_x^2 X + \sum_n U_L(nk_c) \sin(nk_c X) \\ &+ \frac{N\hbar q V_B^2}{2} \int d\omega' [S(q, \omega') - S(-q, -\omega')] \frac{\sin(\omega - \omega')t}{\omega - \omega'} \end{aligned}$$

$$S(q, \omega) = \frac{N\hbar^2 q^2}{2mE_B(q)} \delta(\hbar\omega - E_B(q))$$

$$S \rightarrow S + \delta S_{CP}(q, \omega)$$

CP opens energy gaps



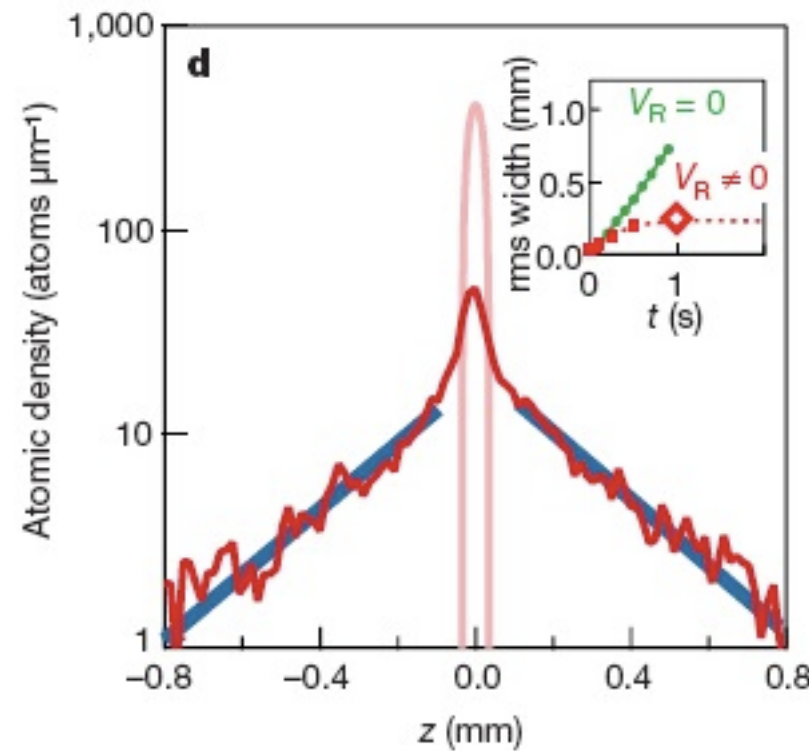
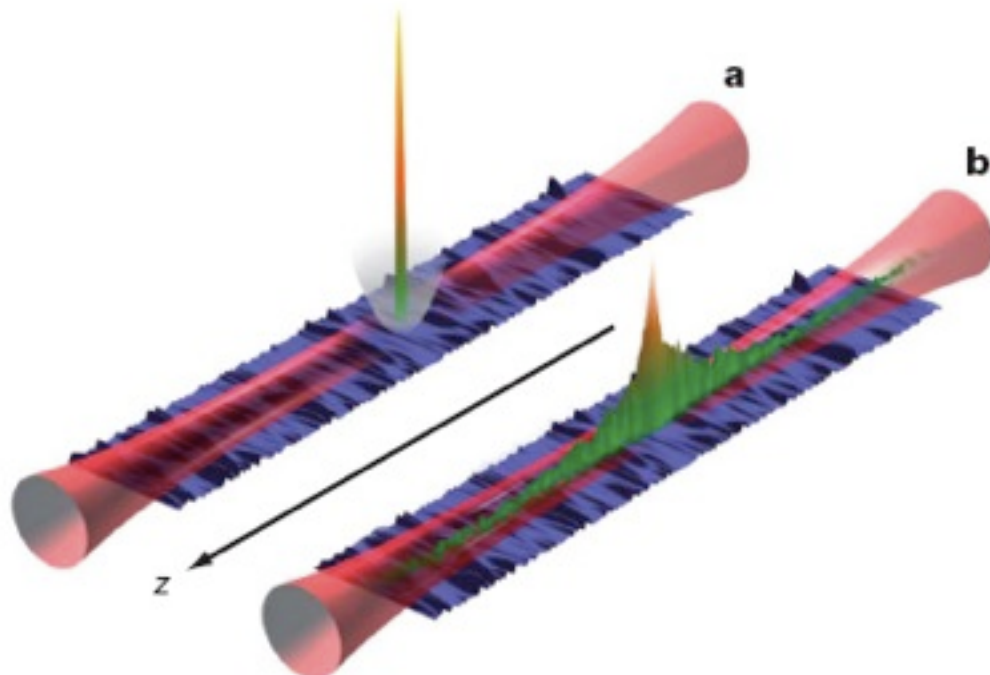
Moreno et al (NJP 2009)

Disorder in quantum vacuum

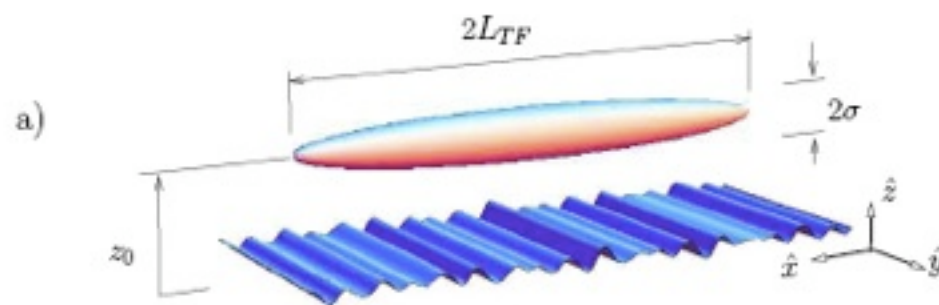


Localization of matter waves

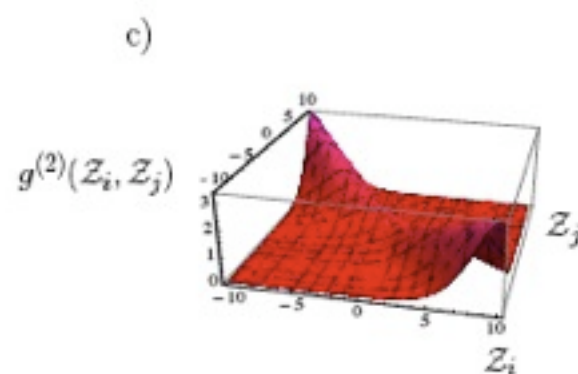
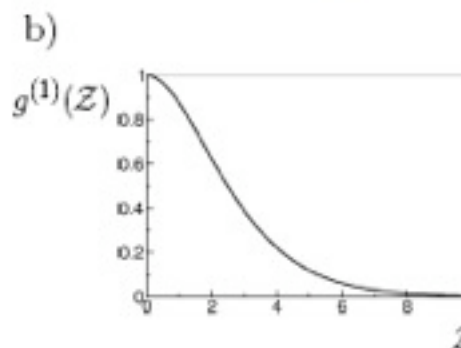
- ⌚ Waves propagating in disordered potentials undergo multiple scattering processes that strongly affect their usual diffusive transport and can result in localized states.
- ⌚ Recently localization of a 1D BEC has been observed: in a speckle potential (Aspect group, 2008) and in a bi-chromatic optical potential (Inguscio group, 2008)



CP for rough surface



$$h(x) = \sum_{i=1}^{\infty} h_i \cos(k_i x + \theta_i)$$



$$U_L^{(1)}(x, z) = -\frac{3\hbar c \alpha(0)}{8\pi^2 \epsilon_0 z^5} \sum_{i=1}^{\infty} h_i g^{(1)}(k_i z) \cos(k_i x + \theta_i), \quad (1)$$

$$\begin{aligned} U_L^{(2)}(x, z) &= -\frac{15\hbar c \alpha(0)}{32\pi^2 \epsilon_0 z^6} \sum_{i,j=1}^{\infty} h_i h_j \\ &\times [\cos((k_i + k_j)x + \theta_i + \theta_j) g^{(2)}(k_i z, k_j z) \\ &+ \cos((k_i - k_j)x + \theta_i - \theta_j) g^{(2)}(k_i z, -k_j z)], \end{aligned} \quad (2)$$

BEC dynamics + weak disorder



GP equation

$$i\hbar \partial_t \varphi(x, t) = -\frac{\hbar^2}{2m} \partial_x^2 \varphi(x, t) + U_L(x, z_0) \Theta(t) \varphi(x, t) \\ + \frac{m\omega_x^2 x^2}{2} \Theta(-t) \varphi(x, t) + g_{\text{eff}} |\varphi(x, t)|^2 \varphi(x, t), \quad (3)$$

Weak disorder:

$$V_R(z_0) \ll \mu \quad V_R^2(z_0) = \overline{(U_L(x, z_0) - \overline{U_L(x, z_0)})^2}$$

short-times: interactions dominant, disorder negligible

large-times: disorder dominant, interactions negligible

$$\overline{n(x)} = \frac{3N\xi}{2} \int_0^{1/\xi} (1 - k^2 \xi^2) \overline{|\phi_k(x)|^2} dk, \quad (4)$$

$$\overline{|\phi_k(x)|^2} = \frac{\pi^2 \gamma(k)}{2} \int_0^\infty u \sinh(\pi u) \\ \times \left(\frac{1+u^2}{1+\cosh(\pi u)} \right)^2 e^{-2(1+u^2)\gamma(k)|x|} du. \quad (5)$$

$\xi = \hbar/\sqrt{4m\mu}$ is the healing length of the BEC

CP disorder correlation

$$C(|x - x'|; z_0) = \overline{U_L(x, z_0) U_L(x', z_0)}^*$$

$$\gamma(k) = \frac{m}{4\hbar^2 E_k} \int_{-\infty}^{\infty} C(x) \cos(2kx) dx$$

$$E_k = \hbar^2 k^2 / 2m$$

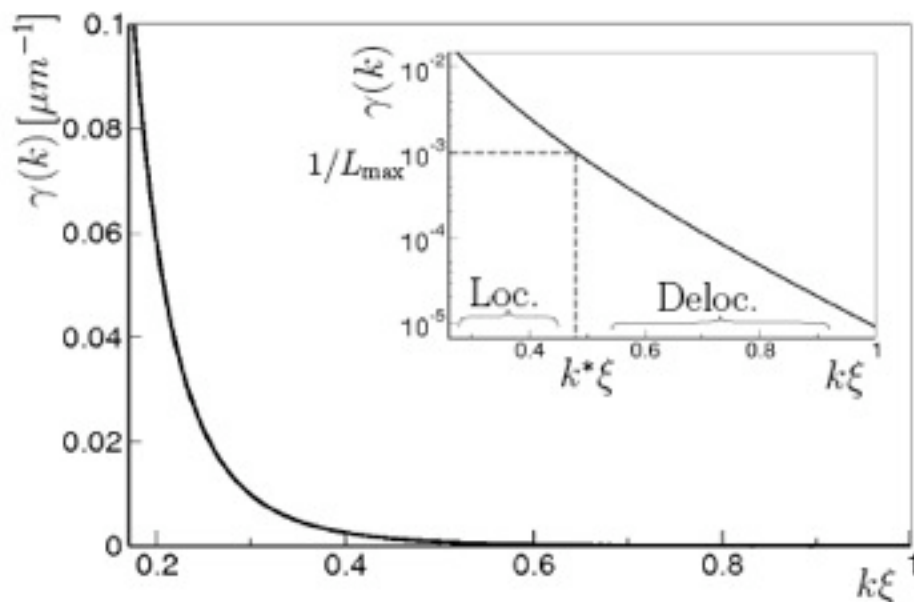


FIG. 2: $\gamma(k)$ vs. $k\xi$ from Eq.(6). The atom-surface distance is $z_0 = 1.5\mu\text{m}$. Inset: same data in Log-Lin scale, the maximum length scale to be measured $L_{\max} = 1\text{mm}$, and the value $k^* = \gamma^{-1}(1/L_{\max})$ separating localized (Loc.) from delocalized (Deloc.) modes.

$$\gamma(k) = \frac{m\pi^2 F^2(z_0)}{2\hbar^2 E_k (2k)^2} \overline{h(x)^2} P(\pi/k) \left(g^{(1)}(2kz_0) \right)^2, \quad (6)$$

$$F(z_0) = 3\hbar c\alpha(0)/8\pi^2\epsilon_0 z_0^5.$$

CP-induced localization

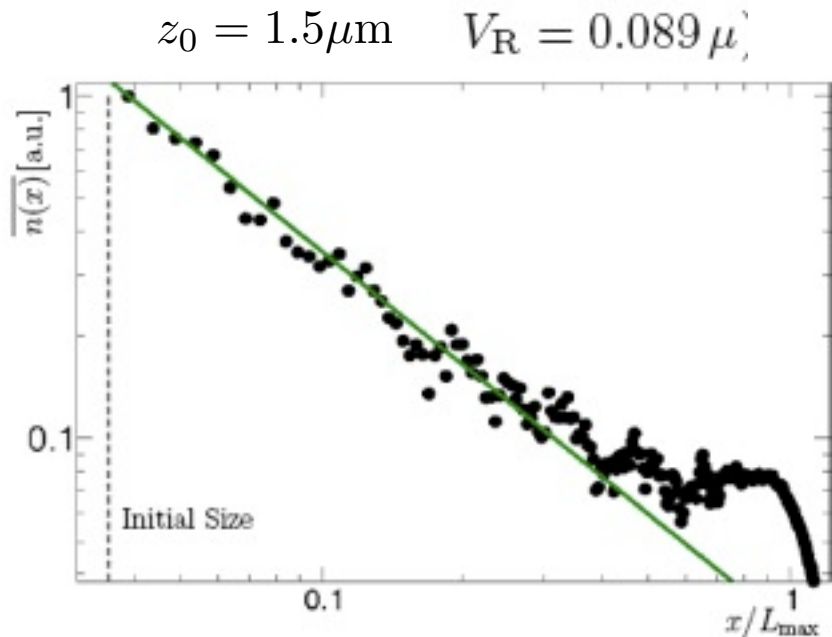


FIG. 3: BEC density (arbitrary units) vs. position. Both the perturbative theory described by Eqs.(4,5,6) (solid) and the full numerical simulation (dots) are computed using the first order approximation for the CP potential at $z_0 = 1.5\mu\text{m}$. The surface profile is averaged over 40 realizations. Time corresponds to $\omega_x t = 28$.

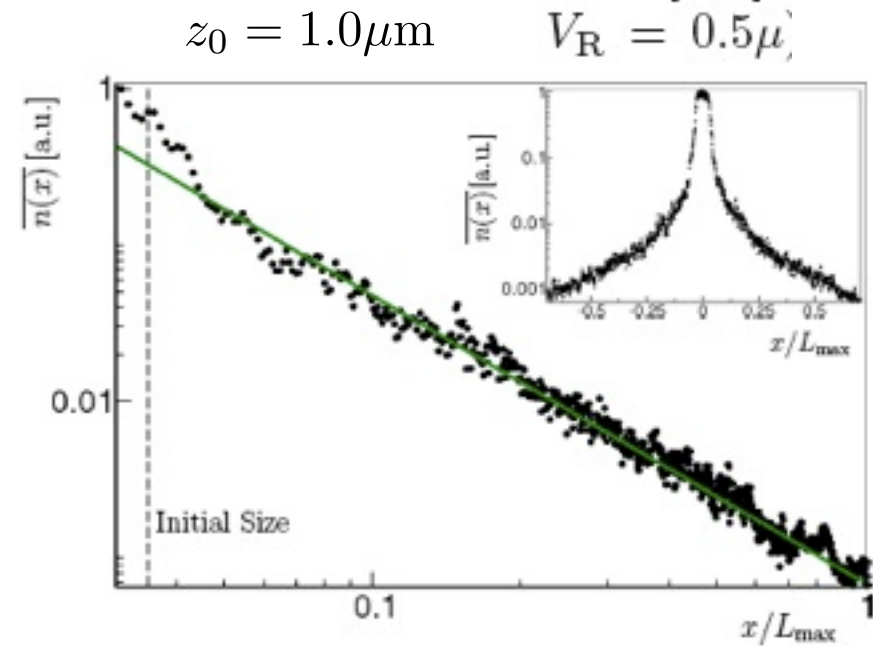


FIG. 4: BEC density (arbitrary units) vs. position, after $\omega_x t = 14$. The profile is averaged over 40 realizations at a distance of $z_0 = 1.0\mu\text{m}$. Numerical simulation (dots) includes both the first and second order terms of the lateral CP potential $U_L(x, z)$. The wing is fitted by a power law $n(x) \propto 1/x^\nu$ with $\nu = 1.84$ (solid). Inset: zoom of the numerical data in Log-Lin scale.

$N = 100$ ^{87}Rb atoms

$\sigma = 0.25\mu\text{m}$ (i.e., radial trapping frequency $\omega_r = 2\pi \times 286\text{Hz}$)

$L_{\text{TF}} = 35\mu\text{m}$ (i.e., $\omega_x = 2\pi \times 2.75\text{Hz}$)

$\xi = 0.85\mu\text{m}$.

$h_i \in [0, 200]\text{nm}$

$\theta_i \in [0, 2\pi]$,

$\lambda_i \in [1, 20]\mu\text{m}$